BIOCHEMISTRY
including biophysical chemistry & molecular biology

Article

pubs.acs.org/biochemistry

Liaison between Myristoylation and Cryptic EF-Hand Motif Confers Ca^{2+} Sensitivity to Neuronal Calcium Sensor-1

Vangipurapu Rajanikanth,[†,∥] Anand Kumar Sharma,[†,∥] Meduri Rajyalakshmi,[†] Kousik Chandra,[‡] Kandala V. R. Chary,[‡,§] and Yogendra Sharma*[,†]

[†]CSIR-Centre for Cellular and Molecular Biology (CCMB), Hyderabad 500007, India

[‡]Tata Institute of Fundamental Research, Homi Bhabha Road, Colaba, Mumbai 400005, India

[§]Center for Interdisciplinary Sciences, Tata Institute of Fundamental Research, Hyderabad 500075, India

Supporting Information

ABSTRACT: Many members of the neuronal calcium sensor (NCS) protein family have a striking coexistence of two characteristics, that is, N-myristoylation and the cryptic EF-1 motif. We investigated the rationale behind this correlation in neuronal calcium sensor-1 (NCS-1) by restoring Ca^{2+} binding ability of the disabled EF-1 loop by appropriate mutations. The concurrence of canonical EF-1 and N-myristoylation considerably decreased the overall Ca^{2+} affinity, conformational flexibility, and functional activation of downstream effecter molecules (i.e., PI4Kβ). Of a particular note, Ca^{2+} induced conformational change (which is the first premise for a CaBP to be considered as sensor) is considerably reduced in myristoylated proteins in which Ca^{2+}-binding to EF-1 is restored. Moreover, Ca^{2+}, which otherwise augments the enzymatic activity of PI4Kβ (modulated by NCS-1), leads to a further decline in the modulated PI4Kβ activity by myristoylated mutants (with canonical EF-1) pointing toward a loss of Ca^{2+} signaling and specificity at the structural as well as functional levels. This study establishes the presence of the strong liaison between myristoylation and cryptic EF-1 in NCS-1. Breaking this liaison results in the failure of Ca^{2+} specific signal transduction to downstream effecter molecules despite Ca^{2+} binding. Thus, the EF-1 disability is a prerequisite in order to append myristoylation signaling while preserving structural robustness and Ca^{2+} sensitivity/specificity in NCS-1.

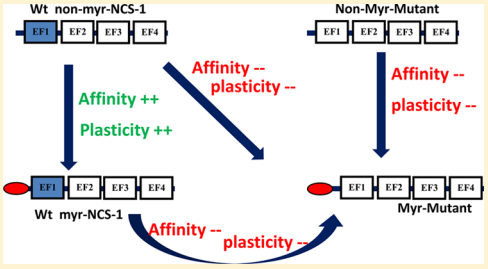

A large subset of the neuronal calcium sensor (NCS) family undergoes a post-translational modification, that is, N-myristoylation. The myristoyl chain thus attached dictates the selectivity and specificity of ligand (Ca^{2+} and Mg^{2+}) binding, cooperativity, and Ca^{2+}-mediated target recognition and signaling of many members of this large superfamily.[1−3] The myristoyl moiety is localized in the vicinity of hydrophobic crevice of EF-1 (EF-hand motifs numbered as EF-1 to EF-4), and is either solvent accessible, as in neuronal calcium sensor-1 (NCS-1),[4] or solvent-inaccessible as seen in recoverin,[5] visinin-like protein-1 (VILIP-1),[6] and guanylate cyclase-activating protein-1 and 2 (GCAP-1 and GCAP-2).[7,8] Some members display Ca^{2+}-induced extrusion of the myristoyl group, which is called as Ca^{2+}-myristoyl switch, demonstrated first in recoverin.[5,9] While this Ca^{2+}-dependent myristoylation switch has been observed in some homologues (VILIP-1, hippocalcin, and neurocalcin-δ), no such switch has been shown in other members (as in NCS-1, GCAP-1).[4,6,8,10,11] We thus broadly categorize these proteins as either "switch" or "nonswitch" members. The domain architecture of these myristoylated NCS proteins comprises, in general, four EF-hand motifs, each with a unique ion binding affinity and selectivity.[8,12−15] Incidentally, at least one of the EF-hand motifs in these proteins is cryptic: one (EF-1) in NCS-1, VILIP1, and GCAP-1 and two (EF-1, EF-4) in recoverin.[16] These cryptic EF-hands lack key amino acid residues needed for Ca^{2+}-coordination. For example, an Asp residue that is usually present at the $+x$ position of a canonical EF-hand loop is replaced by a Lys (or by an Arg in few members) in the EF-1 motif of all the members, thus disabling the motif for binding Ca^{2+}.

Despite the structural and functional variability present among the NCS proteins, there is one remarkable resemblance, that is, concurrent presence of the myristoyl group and the cryptic EF-1 motif placed at the N-terminal region (sequence alignment of the EF-1 region of some selected NCS proteins is shown in Figure 1a). Conservation of coexistence of the myristoyl tail and the cryptic EF-1 motif in these family members has attracted no attention, except for a few studies addressing the issue only of cryptic EF-1 motifs in maintaining the structural integrity and function in GCAP-1, GCAP-2, and recoverin.[17−20] Thus, an answer to the question as to whether there is any association between the N-terminal myristoylation and the disability of the EF-1 motif in these sensors is pivotal toward understanding their structure−function relationship. In this context, we set out to study NCS-1 (also known as frequenin), an ancient, multifunctional regulator, and a nonswitch member of the family, expressed in various genera

Received: September 9, 2014
Revised: January 6, 2015
Published: January 7, 2015

DOI: 10.1021/bi501134g
Biochemistry 2015, 54, 1111−1122

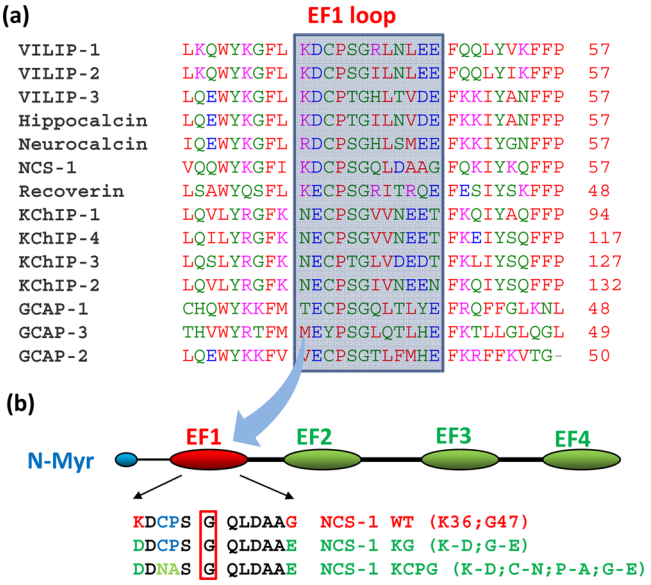

Figure 1. Sequence alignment and strategic point mutations in the EF-1 motif for constructing NCS-1 with restored Ca^{2+} binding to EF-1 motif. (a) Multiple sequence alignment of part of the sequence of NCS proteins showing conserved crypticity of EF-1 in all members of the family. (b) KG mutant: NCS-1 with two mutations as a minimal requirement for a loop to bind Ca^{2+}. KCPG mutant: NCS-1 with four mutations, loop with optimal conformation for Ca^{2+}-binding. Gly at the sixth position of a Ca^{2+}-binding loop is highlighted in the box. Unfavorable residues are marked in red, while mutated favored residues in the EF-1 for Ca^{2+} binding are green. EF-1 motif is marked in red.

and tissues.[2,21] NCS-1 offers obvious advantages of being among the most studied NCS protein, which is also suitable to carry out in vitro activity modulation assay due to a defined constitutive enzyme interacting partner. Despite there being no apparent Ca^{2+}-myristoyl switch in NCS-1, myristoylation influences Ca^{2+}-binding affinity and its pathways.[22,23] Deregulation of its expression has been implicated in various neurodegenerative disorders, for example, schizophrenia, bipolar disorder,[24,25] immature heart function and hypertrophy,[26] and X-linked mental retardation.[27,28] More importantly, being the primordial or founder member of the NCS superfamily, NCS-1 is suitable for understanding not only the involvement of Ca^{2+}-myristoyl chain in protein function but also the evolutionary trend among neuronal calcium sensors.

To figure out the existence of a link between myristoylation and cryptic EF-1 in NCS-1, we replaced strategically placed, nonfavorable residues with favorable Ca^{2+} coordinating residues at +x and −z positions in the Ca^{2+}-binding loop region of cryptic EF-1, restoring its Ca^{2+}-binding ability. We demonstrate that the myristoyl group imposes severe restraint on the conformational transitions emerging from Ca^{2+}-binding when EF-1 is rendered canonical. In other words, despite binding Ca^{2+}, the myristoylated NCS-1 with a noncryptic EF-1 motif no longer senses a Ca^{2+} signal. This work implies that while myristoylation was an adaptive trait for creating specificities of NCS-1, the first EF-hand had to be disabled because of an evolutionary pressure for retaining Ca^{2+} sensitivity.

MATERIALS AND METHODS

Site-Directed Mutagenesis. Required mutations were created in the human NCS-1 gene using Quick-Change mutagenesis kit (Stratagene) and confirmed by gene sequencing. The mutated genes were subcloned into the pET21a vector.

Protein Preparation. Myristoylated and nonmyristoylated NCS-1 proteins were prepared by overexpressing the human cDNA cloned into the pET21a vector as described earlier, with minor modifications.[22,29,30] Proteins were purified by hydrophobic interaction chromatography on a phenyl-Sepharose column. Briefly, the proteins were bound to the column in binding buffer (50 mM Tris, pH 8.5, 100 mM KCl, 1 mM $CaCl_2$, 1 mM $MgCl_2$) and eluted with elution buffer (50 mM Tris, pH 8.5, 3 mM EGTA, 1 mM $MgCl_2$). Gel filtration was employed as a final step of purification. Purified protein fractions were concentrated and rendered Ca^{2+} free by exchange with Chelex-purified buffer in an Amicon ultrafiltration concentrator.

The degree of myristoylation was quantified on a reverse-phase HPLC where relative elution of the myristoylated protein is delayed approximately by 1 min as compared to its nonmyristoylated form.[31] For comparing molecular mass, Analytical size exclusion chromatography setup with a calibrated Superdex 75 column (GE Healthcare) attached to a BioLogic FPLC system (Bio-Rad) was used to compare individual molecular masses of the proteins.

Isothermal Titration Calorimetry (ITC) and Differential Scanning Calorimetry (DSC). Ion-binding affinities were evaluated by ITC experiments at 30 °C on a Microcal VP-ITC instrument. Protein and ligand samples were prepared in Chelex-purified 50 mM Tris, pH 7.5, 100 mM KCl, and 1 mM DTT buffer. All experiments were performed using appropriate concentrations of ligands (generally 3 mM $CaCl_2$ or 10 mM $MgCl_2$). The ITC data thus obtained were baseline corrected and analyzed using the software ORIGIN, supplied with the instrument. The amount of heat released per addition of the titrant was fitted to different models to find out the number of binding sites and the thermodynamic parameters of the protein. For each titration, we performed data fitting with all the models available in the Origin program provided with the instrument. The best fitting model (χ^2 value as well as individual parameters and errors) was considered for obtaining thermodynamic parameters.

DSC data were collected on a VP-DSC microcalorimeter (Microcal Inc.) in the temperature range of 10−100 °C at a rate of 60 °C/h. Appropriate buffer was used to establish the baseline before introducing the protein solution prepared in the same buffer. The protein samples were scanned twice to check the reversibility of the unfolding process. The DSC data were analyzed using the Microcal Origin 7.0 software supplied by the vendor using two-state thermal unfolding model.

Spectral Measurements. Circular dichroism (CD) spectra were recorded on a Jasco J-815 spectropolarimeter, using the appropriate path length cuvettes for near- and far-UV CD. Fluorescence emission spectra were recorded in the correct spectrum mode on an F-4500 Hitachi spectrofluorometer with an excitation wavelength of 295 nm. The excitation and emission band passes were set at 5 nm and spectra of the proteins were recorded in 50 mM Tris (pH 8.5), 100 mM KCl, and 1 mM DTT. Protein hydrophobicity was assessed by ANS fluorescence.

NMR Spectroscopy. NMR spectra were recorded on a BRUKER Avance 800 MHz NMR spectrometer equipped with a cryogenically cooled probe with a pulsed field gradient unit and an actively shielded triple resonance z-gradient probe at

DOI: 10.1021/bi501134g
Biochemistry 2015, 54, 1111−1122

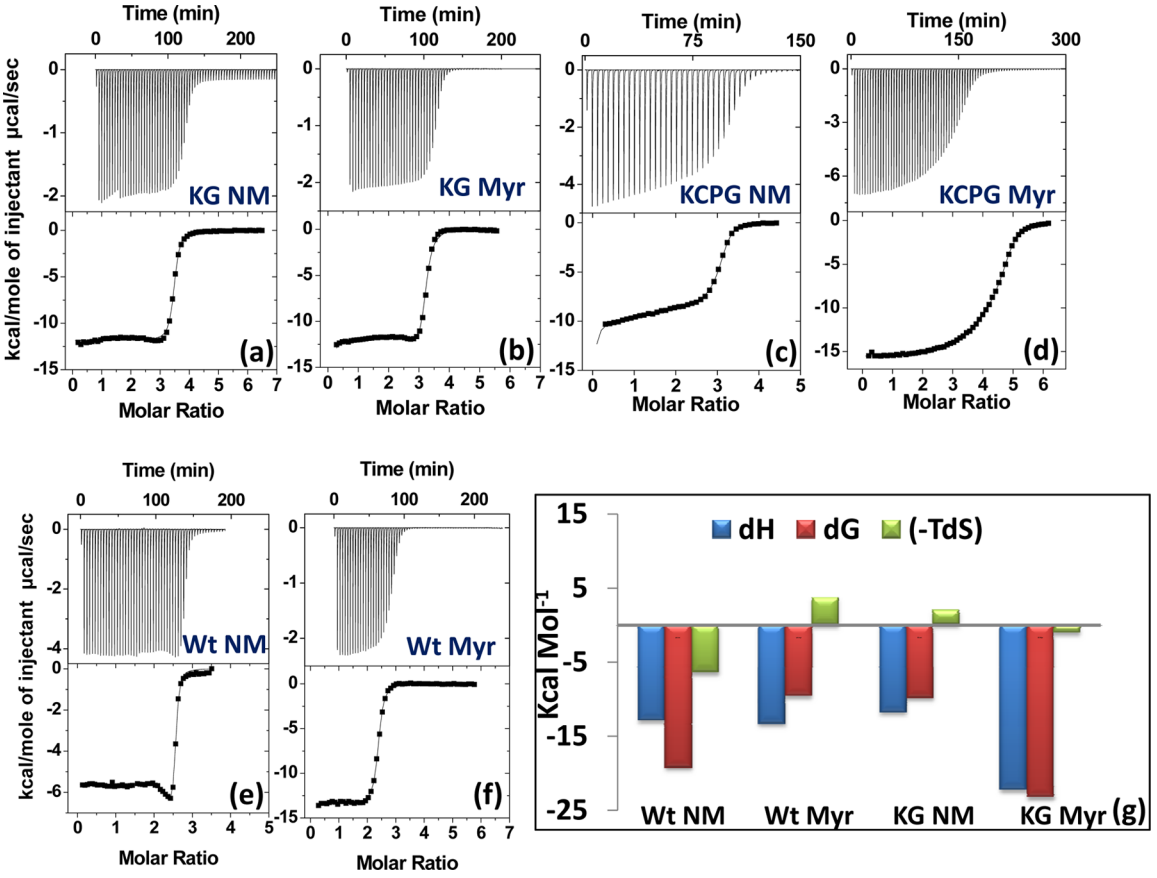

Figure 2. Ca^{2+} binding to different forms of NCS-1 exerts variable effect on the global thermodynamic parameters with a distinct profile of myristoylated KG mutant. (a–f) ITC thermograms of Ca^{2+} titration to myristoylated and nonmyristoylated (abbreviated as Myr and NM, respectively) wt NCS-1, KG and KCPG mutants. (g) Profiles of global free energy, enthalpy, and entropy changes of myristoylated and nonmyristoylated wt, KG mutants upon Ca^{2+} binding.

298 K. While proton chemical shifts were calibrated with respect to 2,2-dimethyl-2-silapentane-5-sulfonate (DSS) at 25 °C (0 ppm), the ^{15}N chemical shifts were calibrated indirectly.[32] The Mg^{2+} titration experiments were carried out by adding small aliquots from a stock solution to 550 μL of 0.8 mM uniformly ^{15}N-labeled protein dissolved in Chelex-treated 50 mM Tris, 100 mM KCl, 1 mM DTT, pH 7.4 buffer taken in a mixed solvent of 90% H_2O and 10% ^2H_2O. After saturation of sample with Mg^{2+}, Ca^{2+} titration was carried out. At each titration point, sensitivity-enhanced 2D [^{15}N,^1H]-HSQC was recorded with the ^1H carrier placed at H_2O resonance (4.7 ppm) and with the ^{15}N carrier at 119 ppm. The experimental time for each of the HSQC spectrum was 40 min with 160 × 2048 complex points along the t_1 and t_2 dimensions, respectively. Quadrature detection in the indirect dimension was achieved using States-TPPI method. The data were processed using TOPSPIN 2.1 software and analyzed using CARA.

Phosphatidylinositol 4-Kinase β (PI4Kβ) Activity Assay. Modulation of lipid kinase activity of target enzyme by different forms of NCS-1 proteins was assayed as the incorporation of radioactive "^{32}P" phosphate group from [γ32-P]ATP as described previously with minor modifications.[33] The reaction mixture (100 μL) contained 50 mM Tris (pH 7.5), 20 mM $MgCl_2$, 1 mM phosphatidylinositol (PI), 0.4% Triton X-100, 100 μM [γ32-P]ATP, 0.5 mg/mL BSA and either 100 μM EGTA (for Ca^{2+}-free assessments) or 3 mM Ca^{2+} (saturating concentration). Each reaction mixture contained 80 μg of PI4Kβ enzyme and varying concentrations of NCS-1 and its different mutants. After mixing all the components, the reaction was started by the addition of [γ32-P]ATP. The reaction was terminated after 15 min by adding 3 mL of $CHCl_3$/CH_3OH/37% HCl (200:100:0.75 (v/v/v). γ32-P phosphorylated lipid was separated from [γ32-P]ATP by mixing 0.6 mL of 0.6% HCl. Finally, 1.5 mL of mixture of $CHCl_3$/CH_3OH/0.6 M HCl in ratio of 3:48:47 (v/v/v) was added to the lower phase followed by mixing and phase separation. Lower phase was transferred to scintillation vials for radioactivity counting in a liquid scintillation counter. After evaporation, the degree of enzymatic activity was measured as a function of radioactivity measured. Experiments were repeated for a minimum of five times for reproducibility with different batches of protein preparation.

Membrane Binding Studies. For the preparation of large unilamellar vesicles (LUVs) of palmitoyl-oleoylphosphatidyl-serine (POPS) lipid, the vacuum-dried, organic solvent free lipid film was soaked in 50 mM Tris, 100 mM KCl, pH 7.5 buffer and incubated at 4 °C for 4–5 h. After brief vortexing, the turbid solution was passed 45 times through a 100 nm polycarbonate membrane with the help of an extruder to make vesicles. Uniformity of vesicle size was checked by dynamic light scattering (DLS) instrument. Total lipid was also extracted from mouse brain by diluting the membrane fraction to organic solvent solution (for 2 mL of aqueous membranous solution, we added 3 mL of 0.5 M KH_2PO4, 15 mL $CHCl_3$, 5 mL CH_3OH) and vacuum-dried, and vesicles were prepared as

DOI: 10.1021/bi501134g
Biochemistry 2015, 54, 1111–1122

Table 1. Ca^{2+}-Binding Affinity and Other Thermodynamic Functions for Mutants Deduced from ITC[a]

NCS-1 mutants (vs Ca^{2+})	model	K_a (M^{-1})	K_d	ΔH (kcal/mol)	ΔS (cal/mol)
wt NM	two-set of sites	K_{a1}: $8.67 \times 10^5 \pm 2.25 \times 10^5$	1.1 μM	$\Delta H1$: -7.303 ± 0.19	$\Delta S1$: 3.08
		K_{a2}: $1.01 \times 10^8 \pm 5.31 \times 10^7$	9.9 nM (106 nM)	$\Delta H2$: -5.627 ± 0.022	$\Delta S2$: 18.1
wt Myr	one-set of sites	K_a ; $8.53 \times 10^6 \pm 4.26 \times 10^5$	117 nM	ΔH: -13.4 ± 0.032	ΔS: −12.5
KG NM	one-set of sites	K_a: $1.32 \times 10^7 \pm 7.90 \times 10^5$	76 nM	ΔH: -11.86 ± 0.026	ΔS: −6.55
KG Myr	four sequential binding sites	K_{a1}: $7.90 \times 10^4 \pm 1.8 \times 10^3$	12.6 μM	$\Delta H1$: -70.26 ± 4.09	$\Delta S1$: −209
		K_{a2}: $1.39 \times 10^6 \pm 3.7 \times 10^4$	719 nM	$\Delta H2$: 87.19 ± 5.72	$\Delta S2$:298
		K_{a3}: $4.09 \times 10^6 \pm 9.3 \times 10^4$	244 nM	$\Delta H3$: $-52x \pm 2.02$	$\Delta S3$: −141
		K_{a4}: 764 ± 26	1.3 mM (7.34 μM)	$\Delta H4$: 12.8 ± 2.88	$\Delta S4$: 55.4
KCPG NM	four sequential binding sites	K_{a1}: $1.05 \times 10^6 \pm 7.8 \times 10^4$	952 nM	$\Delta H1$: 13.99 ± 0.66	$\Delta S1$: 19.63
		K_{a2}: $8.50 \times 10^6 \pm 5.8 \times 10^5$	117 nM	$\Delta H2$: -9.74 ± 1.12	$\Delta S2$: −9.616
		K_{a3}: $1.08 \times 10^7 \pm 6.9 \times 10^5$	92 nM	$\Delta H3$: -4.00 ± 0.66	$\Delta S3$: −9.75
		K_{a4}: $2.27 \times 10^5 \pm 1.2 \times 10^4$	4.4 μM (463 nM)	$\Delta H4$: -0.15 ± 0.06	$\Delta S4$: −7.42
KCPG Myr	two-sets of binding site	K_{a1}: $3.97 \times 10^6 \pm 3.16 \times 10^5$	251 nM	$\Delta H1$: -15.7 ± 0.039	$\Delta S1$: −6.51
		K_{a2}: $3.14 \times 10^5 \pm 2.64 \times 10^4$	3 μM (896 nM)	$\Delta H2$: -8.17 ± 0.529	$\Delta S2$: −5.91

[a]The global K_d was calculated from K_a as inverse of the nth root of $K_{a1} \times K_{a2} \times ... \times K_n$. In the case of the data fittings in multiple binding site models, the global K_d is provided (in parentheses) below the microscopic constants (K_d).

described above for POPS lipid. The protein (2 μM) binding with LUVs was monitored by fluorescence emission. In the case of membrane from mouse brain, the saturating concentration was fixed as one and membrane fraction relative to saturating concentration was plotted against F/F_0; where F_0 and F are the fluorescence intensity at initial (without membrane) and membrane-bound protein, respectively.

RESULTS AND DISCUSSION

Conversion of Cryptic EF-1 Motif to Canonical Motif by Restoring Ca^{2+}-Binding Ability. A synthetic peptide (of 36 amino acids) corresponding to the EF-1 of NCS-1 with two replacements at $+x$ (K36D) and $-z$ (G47E) positions was shown earlier to bind Ca^{2+}, suggesting that this cryptic EF-1 motif can indeed be made to bind Ca^{2+} by these two mutations.[34] We adopted this strategy to convert the cryptic EF-1 of NCS-1 and made the site amenable for Ca^{2+}-binding. NCS-1 with such twin mutations is hereafter referred as KG mutant. To assess redox-dependency, we additionally mutated C38 and P39 to N and A, respectively. NCS-1 with such quadruple mutations, K36D, C38N, P39A, and G47E at positions 1, 3, 4, and 12 of the Ca^{2+}-binding loop, is hereafter referred to KCPG mutant (Figure 1). Proteins with maximum (~100%) myristoylation, as characterized by reverse-phase HPLC, were used in all experiments.

Ca^{2+}-Binding Affinities and Associated Thermodynamic Parameters of NCS-1 Mutants with Restored Ca^{2+} Binding Ability. In addressing the need for the disability of the EF-1 to Ca^{2+} binding, we determined the differences in the Ca^{2+} binding affinities and associated thermodynamic parameters of the wild-type NCS-1 and its two mutants, KG and KCPG (Figure 2a–f). As characterized by the ITC data, both the mutants of NCS-1, KG and KCPG, bind four Ca^{2+} in an exothermic manner. The ITC data for myristoylated KG mutant could be fitted to only a sequential four-site model, with the four macroscopic binding constants as follows: K_{d1} = 12.6 μM, K_{d2} = 719 nM, K_{d3} = 244 nM, and K_{d4} = 1.3 mM) (see Table 1). Out of the four binding sites, two of them have higher Ca^{2+}-binding affinity (in nM range) while the other two exhibit relatively lower affinity (one in mM). The overall (averaged) affinity (calculated as inverse of the fourth root of $K_{a1} \times K_{a2} \times K_{a3} \times K_{a4}$) of myristoylated KG mutant was thus found reduced substantially as compared to that of wt myristoylated NCS-1, which was found to be 117 nM (Figure 2b, Table 1). On the other hand, the nonmyristoylated KG mutant was found to bind Ca^{2+} with an affinity (76 nM) comparable to wt myristoylated NCS-1 (117 nM). Thus, the observed reduction in Ca^{2+} affinity to myristoylated KG mutant is evidently due to the coupling of myristoylation with the canonical EF-1.

Ca^{2+} binding isotherm of myristoylated KCPG mutant (a redox insensitive form of NCS-1, as Cys at the position 38 was mutated to Asn) was sigmoidal and could be best fitted to two-set of binding site model with Ca^{2+}/protein ratio of 4 molar equiv (Figure 2d). The higher affinity set has apparent K_d = ~250 nM (macroscopic binding constant $K_1 = 3.97 \times 10^6$ M^{-1}, ΔH_1 = −15.7 kcal/mol) and the lower affinity set has an apparent K_d = 3 μM (macroscopic binding constant $K_2 = 3.14 \times 10^5$ M^{-1}, ΔH_2 = −8.17 kcal/mol). Overall dissociation constant (K_D) for myristoylated KCPG was found to be 896 nM. Thus, the observed reduction in Ca^{2+}-binding affinity even in the case of myristoylated KCPG mutant as compared to that of wt myristoylated NCS-1 is again attributed to the coupling of myristoylation with the canonical EF-1.

The major conclusion from the ITC data is that the reduction in Ca^{2+}-binding affinity of NCS-1 is caused only if canonical EF-1 is present along with the N-myristoylation. The difference in Ca^{2+} binding and changes thereupon for KG mutant is also witnessed by more relevant and comprehensive thermodynamic parameters, in the form of observed changes in global entropy and enthalpy. The ITC thermodynamic signature graph of Ca^{2+} binding to myristoylated KG mutant (and nonmyristoylated wt form) indicates the involvement of hydrophobic and van der Waals interactions owing to favorable enthalpy change (ΔH) and entropy factor ($T\Delta S$) (Figure 2g). In contrast, nonmyristoylated KG mutant (and wt myristoylated form) exhibit higher extent of Ca^{2+} induced conformational changes (unfavorable entropy change), which is a characteristic of NCS proteins (Figure 2). Since myristoylated

DOI: 10.1021/bi501134g
Biochemistry 2015, 54, 1111−1122

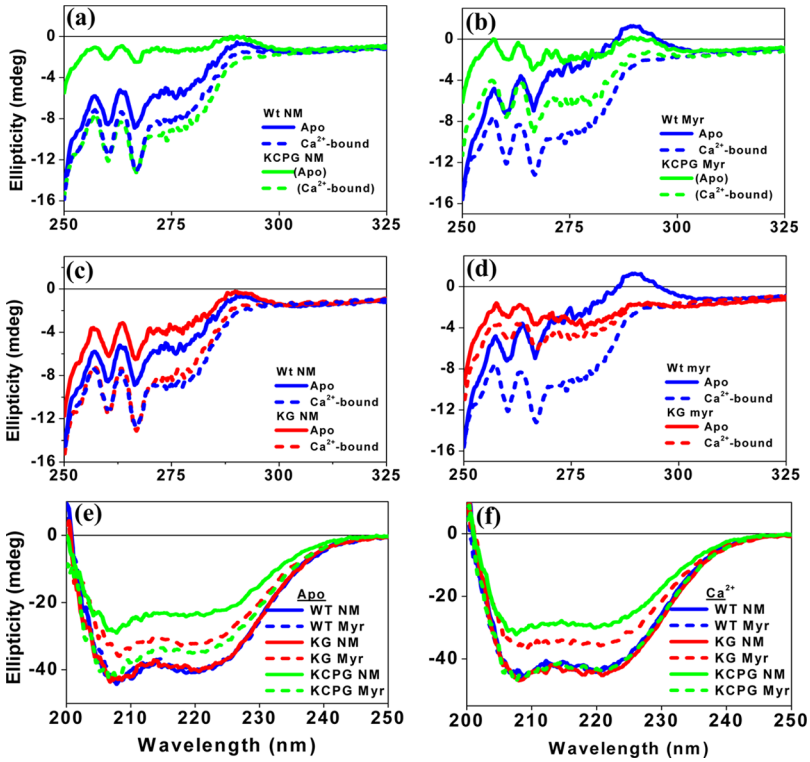

Figure 3. Conformation of myristoylated and nonmyristoylated KG and KCPG mutants in the apo- and holo-forms: Near-UV CD spectra of (a) apo forms of nonmyristoylated wt and KCPG mutants compared with their Ca^{2+}-bound forms. (b) apo forms of myristoylated wt and KCPG mutants and corresponding Ca^{2+}-bound forms. (c) apo and Ca^{2+}-bound forms of nonmyristoylated wt and KG mutant. (d) apo forms of myristoylated wt and KG mutant with their Ca^{2+}-bound form. Far-UV CD spectra of: (e) apo nonmyristoylated (solid lines) and myristoylated (dotted lines) proteins. (f) Ca^{2+} saturated nonmyristoylated (solid lines) and myristoylated (dotted lines) proteins.

NCS-1 is physiologically functional form, the analogous profile (i.e., of nonmyristoylated KG mutant) seems to be closer to its functional form than myristoylated KG mutant where the loss of the liaison results in a thermodynamic profile dissimilar to that of wt myristoylated NCS-1. It demonstrates that the mechanism of Ca^{2+} binding to myristoylated KG mutant is different from that of its nonmyristoylated KG mutant or wt myristoylated NCS-1. This, in turn, implies that the pairing of canonical EF-1 with myristoylation has significant effects on Ca^{2+}-binding properties of NCS-1.

Upon restoring Ca^{2+}-binding to EF-1, all four EF-hand motifs of NCS-1 bind Ca^{2+} and the interaction of myristoyl group, which is located in the vicinity of EF-1, is affected as it attenuates Ca^{2+}-binding affinity ($K_{Ca^{2+}}/K_{apo}$) drastically when compared to its wild-type protein. Myristoylation was shown earlier to induce cooperativity and flexibility to NCS-1 indicating that myristoyl group performs as an allosteric activator of Ca^{2+} binding.[22,35] As is evident from Table 1, the global affinity of the myristoylated mutants is lower than of nonmyristoylated mutant (or wt proteins) (Figure 2, Table 1). Hence, a negative cooperativity is caused by the myristoylation in KG and KCPG mutants. Thus, contrary to wt, the myristoyl group in KG and KCPG mutants becomes an allosteric inhibitor of Ca^{2+} binding, causing a reduction in average/global Ca^{2+} affinity. In calmodulin, Ca^{2+} binding is reported to be driven by enthalpy−entropy compensation with the high affinity C-terminal domain interexchanging the energies with the low affinity N-terminal counterpart, providing the molecule with an open conformation exposing its hydrophobic core.[36] The EF-1 motif in both KG and KCPG mutants is apparently a weaker Ca^{2+} affinity site. Hence, Ca^{2+} may reorganize the mutants in a similar way, in order to exchange energies between the strong and the weaker sites, which in turn could alter the rigidity/flexibility of the molecule.

Cryptic EF-1 Stipulates Ca^{2+} Responsive Conformational Plasticity to Myristoylated NCS-1. NCS-1 undergoes Ca^{2+}-induced conformational change from a closed to open state[37] enabling it to be recognized by its downstream targets. We addressed the question as to whether restoring the Ca^{2+}-binding ability to cryptic EF-1 would affect Ca^{2+}-driven signaling processes of KG and KCPG mutants using near-, and far-UV CD, and NMR spectroscopy, described in the following paragraphs.

(i). Crypticity of EF-1 Loop and Tertiary Structure of the apo Form. The tertiary CD spectral signatures of apo form of myristoylated KG mutant arising from Trp (280−300 nm), Tyr (275−282 nm), and Phe (255−270 nm) regions are significantly less pronounced as compared to the wt counterpart (Figure 3). ^1L_b band at 290 nm, an indicator of the degree of immobilization of Trp, is approximately 2-fold less intense in myristoylated KG mutant than in its nonmyristoylated form, suggesting that the myristoyl group is responsible for the altered microenvironment of Trp and Tyr, while a positive Trp peak (at ∼294 nm) correlates to a possibility of a role of myristoyl group in restricting the mobility of aromatic residues (Figure 3a−d). Supporting this data, myristoylated KG mutant possesses much higher anisotropy in apo form (0.198) than apo nonmyristoylated KG mutant (0.169) or myristoylated wt (0.179) NCS-1. Ca^{2+} binding increases anisotropy in all cases except myristoylated KG mutant (0.1899), further supports the above observations.

DOI: 10.1021/bi501134g
Biochemistry 2015, 54, 1111−1122

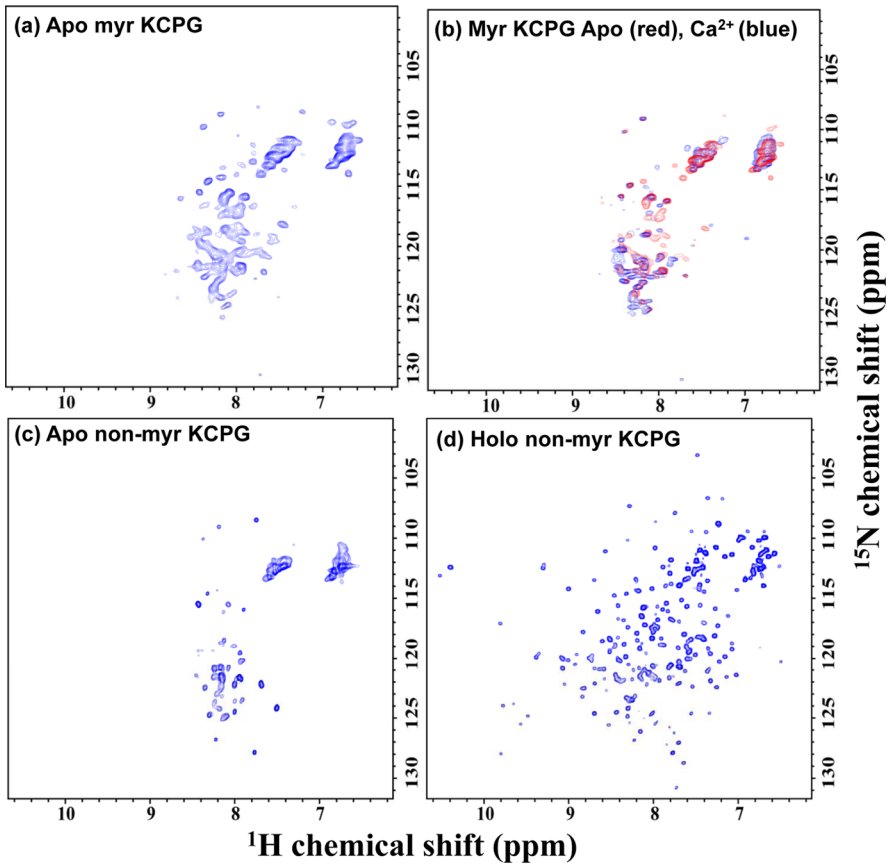

Figure 4. 2D [^{15}N,^{1}H]-HSQC spectra. Myristoylated KCPG mutant: (a) in apo form and (b) in holo form (blue) overlapped with apo form (red). Nonmyristoylated KCPG mutant: (c) in apo form and (d) in Ca^{2+}-bound form is shown for comparison.

Myristoylation of KG mutant reduces the near-UV CD signal (tertiary fold) by approximately 2-fold (in comparison to nonmyristoylated KG mutant or wt myristoylated protein), thereby imposes conformational restraints. Both myristoylated and nonmyristoylated KCPG mutants are comparatively less structured in apo forms as seen in far-UV CD spectra (Figure 3e, f).

(ii). Myristoylation Affects Ca^{2+} Sensitivity When EF-1 Is Activated. As shown in near-UV CD spectra, apo forms of wt myristoylated and nonmyristoylated NCS-1 are in partially unfolded (premolten globule or closed) conformation and attain well-folded (or open) conformation upon binding Ca^{2+} (Figure 3a-d).[37]

In contrast, we obtained unanticipated results with both the myristoylated forms of KG and KCPG mutants. Apo forms of both of these mutants have poor tertiary structural signatures in their near-UV CD spectra (Figure 3b, d). Further, Ca^{2+} titration to wt (myristoylated and nonmyristoylated) and nonmyristoylated KG and KCPG mutants illustrates comparable signals in near-UV CD spectra, the observed changes in ellipticity of myristoylated KG mutants upon addition of Ca^{2+} are less pronounced (Figure 3d). It is interesting to note here that though nonmyristoylated KG mutant shares the key spectral features with wt NCS-1, myristoylated KG mutant shows distinct spectral features. These data together suggest that myristoylation imposes severe restrictions on Ca^{2+}-dependent conformational changes when Ca^{2+} binding ability to EF-1 is restored.

Near-UV CD spectral results that myristoylated KG and KCPG mutants do not undergo equivalent conformational changes upon binding Ca^{2+} were further confirmed by 2D [^{15}N,^{1}H] HSQC spectra, which shows a narrow dispersion of backbone $^{1}H^{N}$ resonances (7.5−8.7 ppm) and accounts for only around 24 peaks out of the expected 173 nonproline peaks (Figure 4), suggesting a poorly folded structure, similar to that of the apo form of wt proteins. Upon binding Ca^{2+}, the number of observed peaks increased to only around 60 with an increased $^{1}H^{N}$ chemical shift dispersion (6.6−8.7 ppm) for both the myristoylated mutants, implying that these mutants did not attain a folded conformation (Figure 4). We may add here that the observed cross-peaks in 2D [^{15}N,^{1}H]-HSQC of the apo and holo mutants were relatively broad with nonuniform line-widths as compared to the cross peaks observed for the apo wt NCS-1.

Similar results were obtained for the nonmyristoylated KG (Figure S1, Supporting Information) and KCPG (Figure 4) mutants, where apo form displays around 40 broad cross-peaks with poor spectral dispersion along the $^{1}H^{N}$ dimension (6.4−8.7 ppm) in the 2D [^{15}N,^{1}H]-HSQC spectra (Figure 4c). However, in the presence of Ca^{2+}, nonmyristoylated KG and KCPG mutants showed all the expected peaks in the 2D [^{15}N, ^{1}H]-HSQC, equal to the number of nonproline residues, with large $^{1}H^{N}$ chemical shift dispersion (6.3−10.8 ppm) (Figure 4d; for 2D [^{15}N,^{1}H]-HSQC spectrum of nonmyristoylated KG mutant, please refer to Figure S1), similar to that seen for the wt nonmyristoylated NCS-1, and supporting the observed results of near-UV CD spectra.[12,22]

Myristoylation-Driven Thermal Stability and Non-cryptic EF-1. As discussed above, both myristoylated mutants bind Ca^{2+} with lower affinity, and undergo modest conforma-

DOI: 10.1021/bi501134g
Biochemistry 2015, 54, 1111−1122

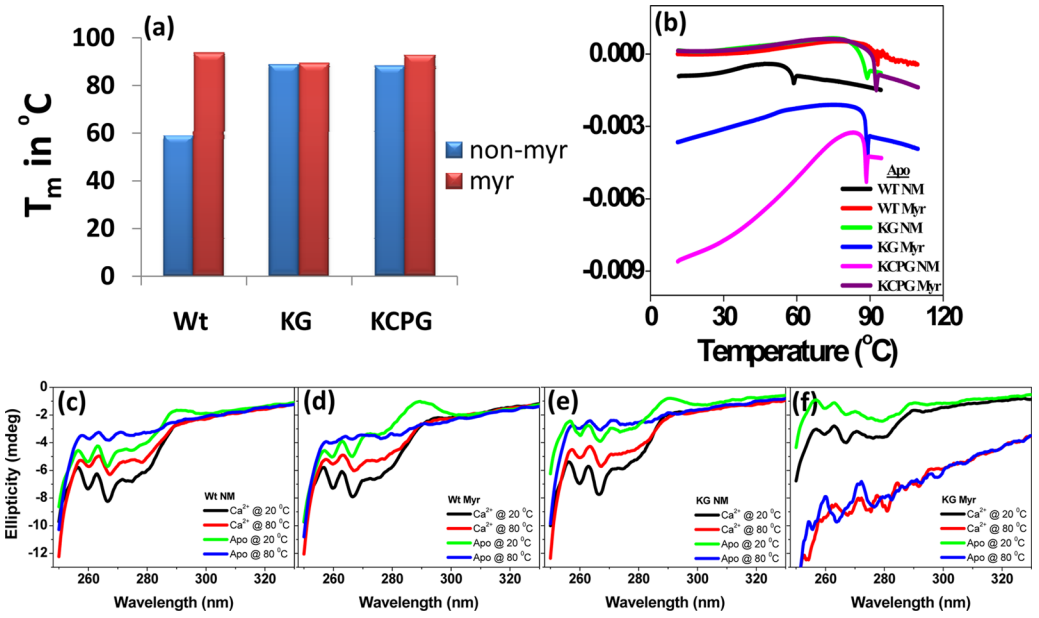

Figure 5. Connection of myristoylation and disabled EF-1 on thermal stability monitored by DSC. (a) A comparison of T_m of apo wt and mutants. (b) Thermal unfolding transitions of wt and KG and KCPG mutants of nonmyristoylated and myristoylated proteins in apo-form (overlapped). (c–f) Near-UV CD spectra of wt and KG mutant (myristoylated and nonmyristoylated) at different temperatures.

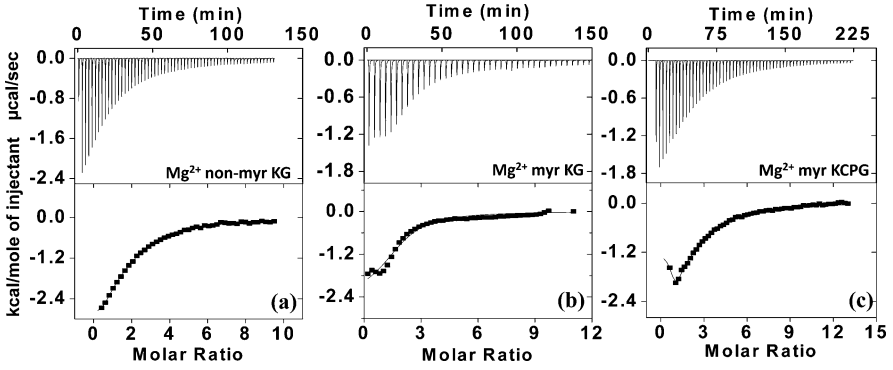

Figure 6. Both KG and KCPG mutants bind Mg^{2+}. ITC analysis of Mg^{2+} binding to (a) nonmyristoylated KG mutant, (b) myristoylated KG mutant, and (c) myristoylated KCPG mutant. Upper panel in thermogram represents the observed heats for each injection of $MgCl_2$ after correcting for heat of dilution, whereas the lower panel depicts the binding enthalpies versus Mg^{2+}/protein molar ratio.

tional changes upon Ca^{2+} binding. Based on these results, we suggest that myristoylation-driven Ca^{2+} sensitivity is reduced when Ca^{2+} binding ability to EF-1 is restored. This liaison between myristoyl group and cryptic EF-1 is also obvious from myristoylation-dependent enhancement of thermal stability (Figure 5). The thermal transition temperatures (T_m) of the apo form of wt nonmyristoylated and myristoylated NCS-1 are 59 and 93 °C, respectively, suggesting that myristoylation enhances thermal stability substantially (from 59 to 93 °C) (Figure 5a). Upon Ca^{2+} binding, T_m of wt nonmyristoylated NCS-1 increases to 83 °C with the precipitation of the protein at higher temperatures, and thus, the thermal unfolding was irreversible. On the other hand, Ca^{2+}-bound wt myristoylated NCS-1 was found to be extremely stable (with an apparent T_m >100 °C) and most importantly, the thermal unfolding was reversible following a two-state thermal unfolding transition without any precipitation (data not presented). In the case of the KG mutant with substitution of Asp and Glu at $+x$ and $-z$ positions, the apparent T_m was found to be 89 and 88 °C for myristoylated and nonmyristoylated mutants, respectively, in their Ca^{2+}-free form (Figure 5). It is interesting to mention that apo-calmodulin is thermally much less stable (T_m about 40 °C)[38] than nonmyristoylated mutants despite being similar in possessing four canonical EF-hand motifs and no myristoylation.

In the Ca^{2+} bound form, the thermal unfolding of all KG mutants follows via an on-pathway folding intermediate with apparent T_m of ∼80 °C and unfolds at ∼100 °C with precipitation (data not presented). On the other hand, further substitution of Cys-Pro residues do not alter the apparent T_m to a greater extent with respect to KG mutant, either in its Ca^{2+}-free or in Ca^{2+}-bound forms, implying no influence of redox system on thermal stability (Figure 5). These findings are supported by thermal unfolding studies monitored by near-UV (Figure 5c-f) and far-UV CD (data not presented). Thus, myristoylation-driven thermal stability of wt NCS-1 is found to be absent in both mutants.

Transformation of Ca^{2+}-Specific (Regulatory) Site to Structural as a Consequence of Noncryptic EF-1. Both the KG and KCPG mutants bind Mg^{2+} with the stoichiometry of ∼1:4 as seen by ITC (Figure 6). This observation suggests a possibility that all the EF-hands (including EF-4 which is a

DOI: 10.1021/bi501134g
Biochemistry 2015, 54, 1111−1122

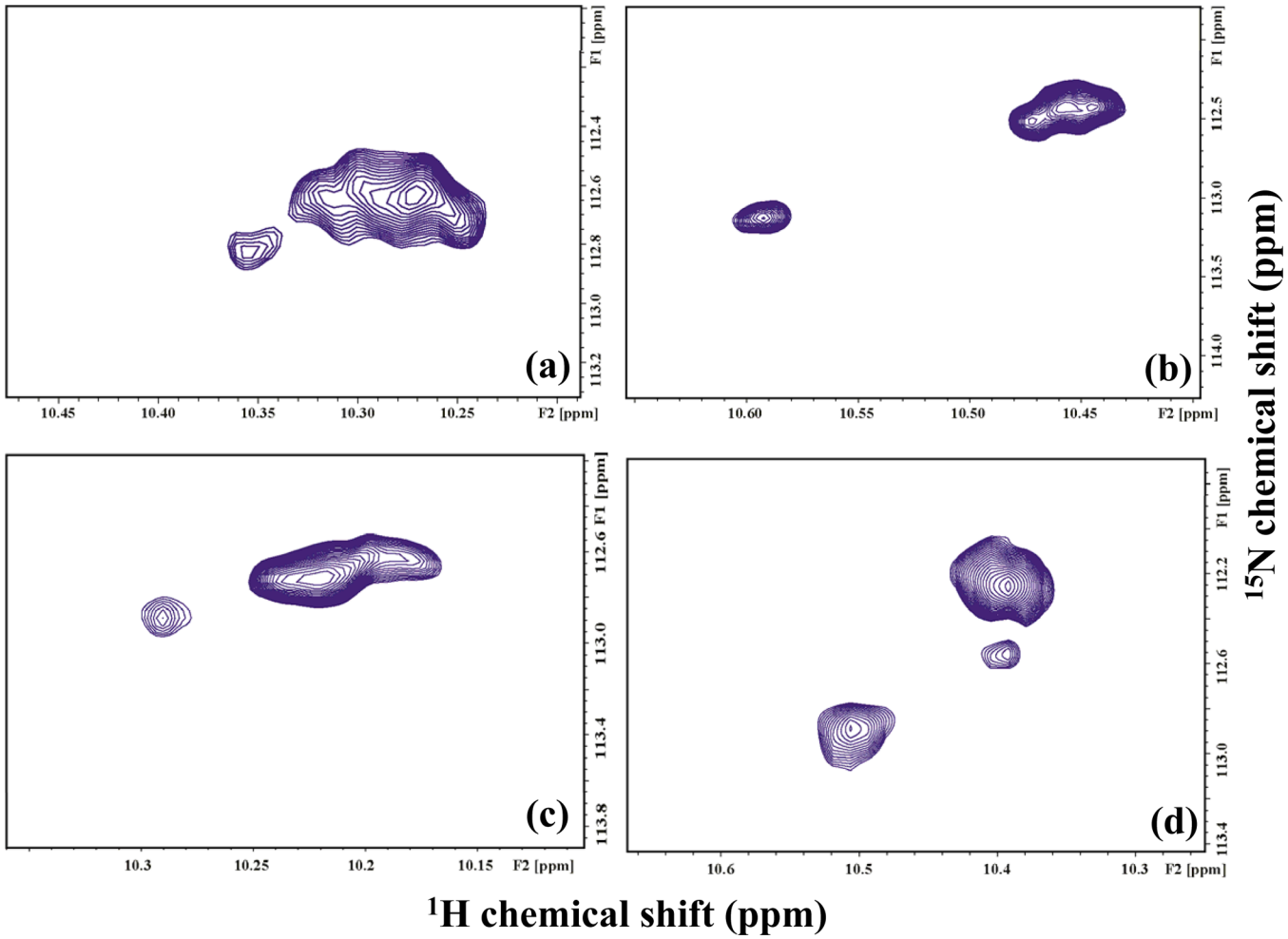

Figure 7. Ca^{2+}-specific (regulatory; EF-4) site is lost to structural (Ca^{2+}/Mg^{2+} binding) site by restoring Ca^{2+} binding ability to EF-1. Unassigned cross peaks of Gly residues present at the 6th position of EF-hand loops as seen in 2D [^{15}N,^{1}H]-HSQC. (a) Mg^{2+}-bound nonmyristoylated KG mutant. (b) Ca^{2+}-saturated nonmyristoylated KG mutant. (c) Mg^{2+}-bound nonmyristoylated KCPG mutant. (d) Ca^{2+}-saturated nonmyristoylated KCPG mutant.

Ca^{2+}-specific site in wt NCS-1) may bind Mg^{2+}. To ascertain the Ca^{2+}/Mg^{2+} discrimination of binding sites in mutants, we employed NMR spectrometry for obtaining spectral signatures of the backbone amide protons ($^{1}H^{N}$) of the conserved Gly residue located at the sixth position of the Ca^{2+}-binding loops (Figure 1b), which exhibits a characteristic downfield shift upon Ca^{2+} or Mg^{2+} binding to the protein in the least crowded region of 2D [^{15}N,^{1}H]-HSQC spectra. In the case of both KG and KCPG mutants, one would expect four (^{15}N,^{1}H) cross peaks arising from the conserved Gly residue at the sixth position of each of the Ca^{2+}-binding loops present in the protein[12] (Figure 1). As shown in panels (a) and (b) of Figure 7, we noticed that broad overlapping peaks arising from Gly residues upon Ca^{2+}/Mg^{2+}-binding could be resolved by employing 60 ms T_2-delay, as these residues were found to possess different transverse relaxation rates (R_2) (Figure 7a, b). Observation of the four cross peaks in this region of HSQC confirms the presence of four Ca^{2+}/Mg^{2+}-binding sites. Thus, all the binding sites are found to be structural in nonmyristoylated KG (Figure 7a, b) and KCPG (Figure 7c, d) mutants, as they bind both Ca^{2+} and Mg^{2+} as also seen by ITC (Figure 6) and none are a Ca^{2+}-specific (or regulatory) site. This is in contrast to wt myristoylated NCS-1, where in EF-2 and EF-3 bind both Ca^{2+} and Mg^{2+} forming structural sites, while EF-4 is a Ca^{2+}-specific or regulatory site.[12] As discussed above, upon binding Ca^{2+}, myristoylated KG mutant undergoes modest conformational changes are rather inappropriate. Due to this, the downfield shifted peaks in 2D [^{15}N,^{1}H]-HSQC could not be resolved even in the Ca^{2+}-bound form of myristoylated KG mutant.

Reduced Modulation of Downstream Target PI4Kβ Activity by Mutants: Antagonistic Acts by Ca^{2+}. Following the observation of the loss of Ca^{2+} specificity and sensitivity by mutations in the EF-1 loop of NCS-1, we addressed the functional consequences of these manipulations. We used the established radiometric enzymatic assay involving the modulation of PI4Kβ activity, which is one of the key regulators of intracellular lipid signaling.[33] PI4Kβ, which is known to form an intracellular complex with NCS-1 and calneurons, is recruited to the Golgi membrane, concomitantly phosphorylating PI to generate phosphatidylinositol 4-phosphate,[39−41] which after another phosphorylation directs the production of InsP3 by phospholipase C. To find out the signaling consequences, we analyzed the ability of the mutants of NCS-1 (with restored Ca^{2+} binding ability to EF-1) in modulating the lipid kinase activity. Though KG mutant in its nonmyristoylated form could augment the enzymatic activity to a greater extent (~3-fold enhancement) than wt nonmyristoylated NCS-1, myristoylated

DOI: 10.1021/bi501134g
Biochemistry 2015, 54, 1111−1122

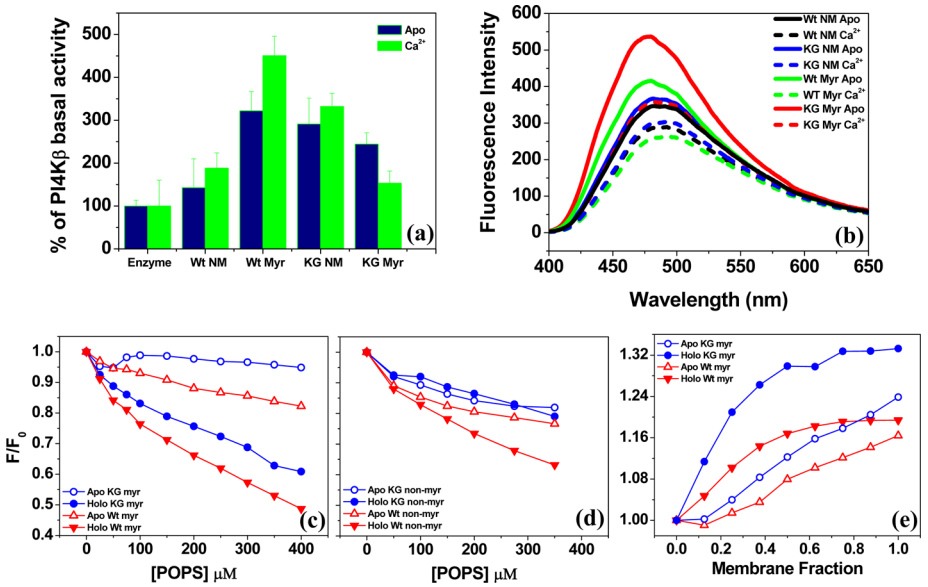

Figure 8. Restoring Ca^{2+} binding to EF-1 diminishes the modulation of PI4Kβ activity by myristoylated NCS-1: Ca^{2+} adversely affects enzymatic activity. (a) Modulation of PI4Kβ activity by wt/mutants of NCS-1 in the presence (green) or absence (blue) of Ca^{2+}. Enzymatic activity in the absence of primary modulator (NCS-1) was considered as basal activity (100%) of PI4Kβ. (b) ANS fluorescence emission spectra of wt and mutant NCS-1 in the absence (solid lines) or the presence (dotted line) of Ca^{2+}. LUVs (of POPS) binding monitored by fluorescence with (c) myristoylated and (d) nonmyristoylated wt and KG mutant. (e) Change in emission maximum of protein upon binding with membrane lipid isolated from mouse brain.

KG mutant stands out against the enhanced positive modulatory efficacy of its nonmyristoylated counterpart (KG mutant) and achieved "net positive modulation" is least among all (<2-fold of the basal activity). As a control, wt myristoylated NCS-1 increases the PI4Kβ activity to a much-elevated level (~4-fold increase in the basal enzymatic activity), while wt nonmyristoylated form enhances the enzymatic activity by ~2-fold, similar to that reported earlier[42] (Figure 8a).

The striking result is the adverse effect of Ca^{2+} on enzyme activation by NCS-1. Wt (both myristoylated and non-myristoylated NCS-1) and nonmyristoylated KG mutant display enhanced modulation (positive) of enzymatic activity by Ca^{2+} as shown earlier in various studies. Conversely, Ca^{2+} acts as a negative modulator of the catalytic cooperativity between myristoylated KG mutant and PI4Kβ, that is, after the addition of Ca^{2+}, modulated enzymatic activity is further reduced (Figure 8a). These observations collectively suggest that the activation of PI4Kβ is dependent on the concurrence of two key features (i.e., myristoylation and cryptic EF-1); breaking this not only leads to the reduced modulation capacity but also inverses the Ca^{2+}-induced effects in the overall enhancement of enzymatic activity of the downstream target.

Redistribution of Surface Hydrophobicity by Functional EF-1: A Determinant of PI4Kβ-NCS-1 Interaction. As surface hydrophobicity of any given protein is one of the key determinants of many protein−protein interactions including PI4Kβ-NCS-1 interaction,[43,44] we examined whether KG and KCPG mutations cause any disparity in surface hydrophobicity of NCS-1 (which may lead to inappropriate interaction with PI4Kβ rendering unregulated, nonoptimal modulation of the enzyme activity as observed in PI4Kβ assay) using 8-anilinonaphthalene 1-sulfonate (ANS). Myristoylated proteins (both wt and mutants) have substantially higher ANS fluorescence than that of nonmyristoylated counterpart (Figure 8b). This increased emission intensity, for instance, can be assumed as an attribute of myristoyl group, but at the same time, fluorescence intensity of ANS complexed with non-myristoylated KG mutant being comparable to ANS with wt myristoylated NCS-1, signifies the more exposed hydrophobic patches after mutations. Interestingly, the relative emission intensity of ANS-myristoylated KG mutant was 25% higher (than ANS-wt myristoylated NCS-1). Considering the fact that Ca^{2+} leads to reduced fluorescence of ANS complexed with wt protein, Ca^{2+} did not influence surface hydrophobicity of myristoylated KG mutant up to the level that is seen in wt myristoylated protein (Figure 8b). NCS-1 being a membrane associated protein in cells, we examined the membrane association propensity of NCS-1 and its reactivated EF-1 KG mutants. We observed that Ca^{2+} bound myristoylated KG mutant has higher affinity for lipid than its apo form as also for myristoylated wt NCS-1[22] (Figure 8c−e). On the other hand, binding of nonmyristoylated proteins is comparatively much less, as also reported earlier[22] (Figure 8c, d). Binding was also assessed with the lipid isolated from mouse brain. We observed that, in contrast to slightly less binding of KG mutant (than wt) to POPS vesicles, myristoylated KG mutant binds slightly better to the natural lipid (Figure 8e). Thus, the changes observed in the case of POPS membrane are not considerable and membrane binding propensity of KG mutant is grossly similar to that of wt NCS-1. Hence, the changes observed so far are not due to any aberrant structural change caused by mutation in the protein.

Upon comparing the results of PI4Kβ activation with ANS fluorescence, we observe a trend where a reduction in hydrophobicity of the protein correlates with an increase in the enzyme activation, and vice versa. This observation persuades us to propose that the interaction of PI4Kβ with NCS-1 might be influenced by surface hydrophobicity of NCS-1. Ca^{2+} induced conformational changes lead to the alteration in surface hydrophobicity to facilitate the interaction, while the archetypal EF-1 demises this Ca^{2+} regulated hydrophobicity

DOI: 10.1021/bi501134g
Biochemistry 2015, 54, 1111−1122

switch, resulting in a nonoptimal interaction between the enzyme and its modulator.

CONCLUSIONS

Cryptic EF-1 Is Required for Myristoylation-Dependent Ca^{2+}-Signaling in NCS-1. We initiated this work with a key question: why does NCS-1 have N-myristoylation along with a cryptic EF-1 motif? Based on our results described above, we conclude that myristoylated KG and KCPG mutants (EF-1 with restored Ca^{2+} binding ability) do not undergo the optimal conformational rearrangement upon Ca^{2+}-binding and, therefore, do not "sense" Ca^{2+} hindering downstream signaling. Thus, our data demonstrate that myristoylation regulates the Ca^{2+}-induced conformational transition, only if EF-1 is cryptic. In other words, if Ca^{2+} binding ability to EF-1 is restored, the myristoylated NCS-1 ceases to act as Ca^{2+} sensor, due to an inadequate (or may be inappropriate) conformational transition by Ca^{2+}.

NCS members are considered the evolutionary descendents of primordial calmodulin. While myristoylation was a need for their adaptive evolution, the first EF-hand motif in canonical form would inhibit protein function, as there would be no Ca^{2+} sensitivity in terms of appropriate conformational transitions required for a sensor. For overcoming this, it became imperative to specifically disable the first EF-hand motif, attained by a simple strategy of replacing generally favored residues (Lys to Asp at $+x$ position, and Gly to Glu at $-z$-position) acquired by some myristoylated proteins to remain Ca^{2+} sensor while adding one more feature, i.e., N-myristoylation, for specific interaction with downstream targets. Lys (of the EF loop), when replaced by Asp, changes the surface electrostatics of the protein, and thus gives a more believable explanation for causing the loss of function by myristoyl-electrostatic switch and its positional specificity in membrane proteins topology lend credence to our hypothesis.[45−48] Thus, the conserved Lys36 is critical, as while providing positive charge it disables the loop, whose role needs to be examined in other NCS members as this residue might hold a place of a key controller which does not maintain just the structural integrity of a sensor protein.

In summary, we put forward an essential aspect of some of the members of NCS family, that is., a nexus between myristoylation and cryptic EF-1, which was not addressed before, despite its conservation in this widespread superfamily represented by several sequences reported in the database from various organisms. With NCS-1 being a nonswitch protein, influence of such conversion of EF-1 on myristoylation-driven Ca^{2+} sensing need to be extended to Ca^{2+}-myristoyl switch proteins (possibility of a key control on Ca^{2+}-myristoyl switch) for studying their myristoylation adaptation for fine-tuning and refined functioning at the cost of the first noncryptic EF-hand motif. Additionally, it would be interesting to explore the effect of such mutations in other members of the family, such as neurocalcin (protein with Ca^{2+}-myristoyl switch) and KChIP2/3, which do not have N-myristoylation but still have a cryptic EF-1 motif.

ASSOCIATED CONTENT

Supporting Information

Figure S1 showing 2D[^{15}N,^{1}H]-HSQC spectra of nonmyristoylated KG and KCPG mutants in the Ca^{2+} (a and b) and Mg^{2+} (c and d) bound form. This material is available free of charge via the Internet at http://pubs.acs.org.

AUTHOR INFORMATION

Corresponding Author

*Mailing address: CSIR-Centre for Cellular and Molecular Biology (CCMB), Uppal Road, Hyderabad-500 007, India. Telephone: +91-40-27192561. Fax: +91-40-27160591. E-mail: yogendra@ccmb.res.in.

Author Contributions

‖V.R. and A.K.S. are the joint first authors.

Funding

This work was supported by a Neuroscience grants of Department of Biotechnology (Govt of India), and by the CSIR XII 5-year network grant to Y.S. V.R. and A.K.S. were supported by the Department of Biotechnology (DBT-PDF) and JRF (UGC), respectively. K.V.R.C. acknowledges the J. C. Bose Fellowship of the Department of Science and Technology (DST), Govt of India.

Notes

The authors declare no competing financial interest.

ACKNOWLEDGMENTS

The National Facility for High Field NMR, supported by the Department of Science and Technology, Department of Biotechnology, Council of Scientific and Industrial Research, and Tata Institute of Fundamental Research, Mumbai, is gratefully acknowledged. Thanks to E. Bhikshapathi, V. Krishna Kumari, and C. Subbalakshmi for their help in membrane binding experiments. We acknowledge P. Aravind for his initial experiments, Anant Patel for help in recording some NMR experiments, and Andreas Jeromin (University of Texas at Austin) for discussion.

ABBREVIATIONS

ANS, 8-anilino-1-naphthalene sulfonic acid; CD, circular dichroism; EF-1 to EF-4, EF-hand motifs 1 to 4 of NCS-1; GCAP, guanylate cyclase-activating protein; GdmCl, guanidinium chloride; NCS-1, neuronal calcium sensor-1; PI4Kβ, phosphatidylinositol 4-kinase β; PI, phosphatidylinositol; POPS, palmitoyl-oleoylphosphatidylserine

REFERENCES

(1) Burgoyne, R. D., and Weiss, J. L. (2001) The neuronal calcium sensor family of Ca^{2+}-binding proteins. *Biochem. J. 353*, 1−12.

(2) Ames, J. B., and Lim, S. (2012) Molecular structure and target recognition of neuronal calcium sensor proteins. *Biochim. Biophys. Acta 1820*, 1205−1213.

(3) Ames, J. B., Lim, S., and Ikura, M. (2012) Molecular structure and target recognition of neuronal calcium sensor proteins. *Front. Mol. Neurosci. 5*, 10.

(4) O'Callaghan, D. W., and Burgoyne, R. D. (2004) Identification of residues that determine the absence of a Ca^{2+}/myristoyl switch in neuronal calcium sensor-1. *J. Biol. Chem. 279*, 14347−14354.

(5) Zozulya, S., and Stryer, L. (1992) Calcium-myristoyl protein switch. *Proc. Natl. Acad. Sci. U. S. A. 89*, 11569−11573.

(6) Li, C., Pan, W., Braunewell, K. H., and Ames, J. B. (2011) Structural analysis of Mg^{2+} and Ca^{2+} binding, myristoylation, and dimerization of the neuronal calcium sensor and visinin-like protein 1 (VILIP-1). *J. Biol. Chem. 286*, 6354−6366.

(7) Hwang, J. Y., and Koch, K. W. (2002) Calcium- and myristoyl-dependent properties of guanylate cyclase-activating protein-1 and protein-2. *Biochemistry 41*, 13021−13028.

DOI: 10.1021/bi501134g
Biochemistry 2015, 54, 1111−1122

(8) Lim, S., Peshenko, I., Dizhoor, A., and Ames, J. B. (2009) Effects of Ca^{2+}, Mg^{2+}, and myristoylation on guanylyl cyclase activating protein 1 structure and stability. *Biochemistry 48*, 850−862.
(9) Ames, J. B., Ishima, R., Tanaka, T., Gordon, J. I., Stryer, L., and Ikura, M. (1997) Molecular mechanics of calcium-myristoyl switches. *Nature 389*, 198−202.
(10) Béven, L., Adenier, H., Kichenama, R., Homand, J., Redeker, V., Le Caer, J. P., Ladant, D., and Chopineau, J. (2001) Ca^{2+}-myristoyl switch and membrane binding of chemically acylated neurocalcins. *Biochemistry 40*, 8152−8160.
(11) Stephen, R., Bereta, G., Golczak, M., Palczewski, K., and Sousa, M. C. (2007) Stabilizing function for myristoyl group revealed by the crystal structure of a neuronal calcium sensor, guanylate cyclase-activating protein 1. *Structure 15*, 1392−1402.
(12) Aravind, P., Chandra, K., Reddy, P. P., Jeromin, A., Chary, K. V., and Sharma, Y. (2008) Regulatory and structural EF-hand motifs of neuronal calcium sensor-1: Mg^{2+} modulates Ca^{2+} binding, Ca^{2+}-induced conformational changes, and equilibrium unfolding transitions. *J. Mol. Biol. 376*, 1100−1115.
(13) Alekseev, A. M., Shulga-Morskoy, S. V., Zinchenko, D. V., Shulga-Morskaya, S. A., Suchkov, D. V., Vaganova, S. A., Senin, I. I., Zargarov, A. A., Lipkin, V. M., Akhtar, M., and Philippov, P. P. (1998) Obtaining and characterization of EF-hand mutants of recoverin. *FEBS Lett. 440*, 116−118.
(14) Permyakov, S. E., Cherskaya, A. M., Senin, I. I., Zargarov, A. A., Shulga-Morskoy, S. V., Alekseev, A. M., Zinchenko, D. V., Lipkin, V. M., Philippov, P. P., Uversky, V. N., and Permyakov, E. A. (2000) Effects of mutations in the calcium-binding sites of recoverin on its calcium affinity: Evidence for successive filling of the calcium-binding sites. *Protein Eng. 13*, 783−790.
(15) Senin, I. I., Vaganova, S. A., Weiergräber, O. H., Ergorov, N. S., Philippov, P. P., and Koch, K. W. (2003) Functional restoration of the Ca^{2+}-myristoyl switch in a recoverin mutant. *J. Mol. Biol. 330*, 409−418.
(16) McCue, H. V., Haynes, L. P., and Burgoyne, R. D. (2010) The diversity of calcium sensor proteins in the regulation of neuronal function. *Cold. Spring Harbor Perspect. Biol. 2*, a004085.
(17) Olshevskaya, E. V., Boikov, S., Ermilov, A., Krylov, D., Hurley, J. B., and Dizhoor, A. M. (1999) Mapping functional domains of the guanylate cyclase regulator protein. GCAP-2. *J. Biol. Chem. 274*, 10823−10832.
(18) Ermilov, A. N., Olshevskaya, E. V., and Dizhoor, A. M. (2001) Instead of binding calcium, one of the EF-hand structures in guanylyl cyclase activating protein-2 is required for targeting photoreceptor guanylyl cyclase. *J. Biol. Chem. 276*, 48143−48148.
(19) Hwang, J. Y., Schlesinger, R., and Koch, K. W. (2004) Irregular dimerization of guanylate cyclase-activating protein 1 mutants causes loss of target activation. *Eur. J. Biochem. 271*, 3785−3793.
(20) Permyakov, S. E., Zernii, E. Y., Knyazeva, E. L., Denesyuk, A. I., Nazipova, A. A., Kolpakova, T. V., Zinchenko, D. V., Philippov, P. P., Permyakov, E. A., and Senin, I. I. (2012) Oxidation mimicking substitution of conservative cysteine in recoverin suppresses its membrane association. *Amino Acids 42*, 1435−1442.
(21) Pongs, O., Lindemeier, J., Zhu, X. R., Theil, T., Engelkamp, D., Krah-Jentgens, I., Lambrecht, H. G., Koch, K. W., Schwemer, J., Rivosecchi, R., and Ferrus, A. (1993) Frequenin - A novel calcium-binding protein that modulates synaptic efficacy in the Drosophila nervous system. *Neuron 11*, 15−28.
(22) Jeromin, A., Muralidhar, D., Parameswaran, M. N., Roder, J., Fairwell, T., Scarlata, S., Dowal, L., Mustafi, S. M., Chary, K. V., and Sharma, Y. (2004) N-Terminal myristoylation regulates calcium-induced conformational changes in neuronal calcium sensor-1. *J. Biol. Chem. 279*, 27158−27167.
(23) Chandra, K., Ramakrishnan, V., Sharma, Y., and Chary, K. V. (2011) N-Terminal myristoylation alters the calcium binding pathways in neuronal calcium sensor-1. *J. Biol. Inorg. Chem. 16*, 81−95.
(24) Koh, P. O., Undie, A. S., Kabbani, N., Levenson, R., Goldman-Rakic, P. S., and Lidow, M. S. (2003) Up-regulation of neuronal calcium sensor-1 (NCS-1) in the prefrontal cortex of schizophrenic and bipolar patients. *Proc. Natl. Acad. Sci. U. S. A. 100*, 313−317.
(25) Torres, K. C., Souza, B. R., Miranda, D. M., Sampaio, A. M., Nicolato, R., Neves, F. S., Barros, A. G., Dutra, W. O., Gollob, K. J., Correa, H., and Romano-Silva, M. A. (2009) Expression of neuronal calcium sensor-1 (NCS-1) is decreased in leukocytes of schizophrenia and bipolar disorder patients. *Prog. Neuropsychopharmacol. Biol. Psychiatry 33*, 229−234.
(26) Nakamura, T. Y., Jeromin, A., Mikoshiba, K., and Wakabayashi, S. (2011) Neuronal calcium sensor-1 promotes immature heart function and hypertrophy by enhancing Ca^{2+} signals. *Circ. Res. 109*, 512−523.
(27) Bahi, N., Friocourt, G., Carrié, A., Graham, M. E., Weiss, J. L., Chafey, P., Fauchereau, F., Burgoyne, R. D., and Chelly, J. (2003) IL1 receptor accessory protein like, a protein involved in X-linked mental retardation, interacts with neuronal calcium sensor-1 and regulates exocytosis. *Hum. Mol. Genet. 12*, 1415−1425.
(28) Bai, J., He, F., Novikova, S. I., Undie, A. S., Dracheva, S., Haroutunian, V., and Lidow, M. S. (2004) Abnormalities in the dopamine system in schizophrenia may lie in altered levels of dopamine receptor-interacting proteins. *Biol. Psychiatry 56*, 427−440.
(29) Fisher, J. R., Sharma, Y., Iuliano, S., Piccioti, R. A., Krylov, D., Hurley, J., Roder, J., and Jeromin, A. (2000) Purification of myristoylated and nonmyristoylated neuronal calcium sensor-1 using single-step hydrophobic interaction chromatography. *Protein Expression Purif. 20*, 66−72.
(30) De Cotiis, D. A., Woll, M. P., Fox, T. E., Hill, R. B., Levenson, R., and Flanagan, J. M. (2008) Optimized expression and purification of myristoylated human neuronal calcium sensor-1 in *E. coli*. *Protein Expression Purif. 61*, 103−112.
(31) Desmeules, P., Penney, S. E., and Salesse, C. (2006) Single-step purification of myristoylated and nonmyristoylated recoverin and substrate dependence of myristoylation level. *Anal. Biochem. 349*, 25−32.
(32) Wishart, D. S., Bigam, C. G., Yao, J., Abildgaard, F., Dyson, H. J., Oldfield, E., Markley, J. L., and Sykes, B. D. (1995) 1H, 13C and 15N chemical shift referencing in biomolecular NMR. *J. Biomol. NMR 6*, 135−140.
(33) Nakanishi, S., Catt, K. J., and Balla, T. (1995) Wortmannin-sensitive phosphatidylinositol 4-kinase that regulates hormone-sensitive pools of inositol phospholipid. *Proc. Natl. Acad. Sci. U. S. A. 92*, 5317−5321.
(34) Muralidhar, D., Jobby, M. K., Jeromin, A., Roder, J., Thomas, F., and Sharma, Y. (2004) Calcium and chlorpromazine binding to the EF-hand peptides of neuronal calcium sensor-1. *Peptides 25*, 909−917.
(35) Muralidhar, D., Jobby, M. K., Kannan, K., Annapurna, V., Chary, K. V. R., Jeromin, A., and Sharma, Y. (2005) Equilibrium unfolding of neuronal calcium sensor-1: N-Terminal myristoylation influences unfolding and reduces the protein stiffening in the presence of calcium. *J. Biol. Chem. 280*, 15569−15578.
(36) Gilli, R., Lafitte, D., Lopez, C., Kilhoffer, M., Makarov, A., Briand, C., and Haiech, J. (1998) Thermodynamic analysis of calcium and magnesium binding to calmodulin. *Biochemistry 37*, 5450−5456.
(37) Cox, J. A., Durussel, I., Comte, M., Nef, S., Nef, P., Lenz, S. E., and Gundelfinger, E. D. (1994) Cation binding and conformational changes in VILIP and NCS-1, two neuron-specific calcium-binding proteins. *J. Biol. Chem. 269*, 32807−32813.
(38) Guerini, D., and Krebs, J. (1983) Influence of temperature and denaturing agents on the structural stability of calmodulin. A ^{1}H-nuclear magnetic resonance study. *FEBS Lett. 164*, 105−110.
(39) Mikhaylova, M., Reddy, P. P., Munsch, T., Landgraf, P., Suman, S. K., Smalla, K. H., Gundelfinger, E. D., Sharma, Y., and Kreutz, M. R. (2009) Calneurons provide a calcium threshold for trans-Golgi network to plasma membrane trafficking. *Proc. Natl. Acad. Sci. U. S. A. 106*, 9093−9098.
(40) Zhao, X., Várnai, P., Tuymetova, G., Balla, A., Tóth, Z. E., Oker-Blom, C., Roder, J., Jeromin, A., and Balla, T. (2001) Interaction of neuronal calcium sensor-1 (NCS-1) with phosphatidylinositol 4-kinase

DOI: 10.1021/bi501134g
Biochemistry 2015, 54, 1111−1122

beta stimulates lipid kinase activity and affects membrane trafficking in COS-7 cells. *J. Biol. Chem. 276*, 40183−40189.
(41) Strahl, T., Huttner, I. G., Lusin, J. D., Osawa, M., King, D., Thorner, J., and Ames, J. B. (2007) Structural insights into activation of phosphatidylinositol 4-kinase (Pik1) by yeast frequenin (Frq1). *J. Biol. Chem. 282*, 30949−30959.
(42) Haynes, L. P., Thomas, G. M., and Burgoyne, R. D. (2005) Interaction of neuronal calcium sensor-1 and ADP-ribosylation factor 1 allows bidirectional control of phosphatidylinositol 4-kinase beta and trans-Golgi network-plasma membrane traffic. *J. Biol. Chem. 280*, 6047−6054.
(43) Young, L., Jernigan, R. L., and Covell, D. G. (1994) A role for surface hydrophobicity in protein-protein recognition. *Protein Sci. 3*, 717−729.
(44) Chothia, C., and Janin, J. (1975) Principles of protein-protein recognition. *Nature 256*, 705−708.
(45) Kaplan, J. M., Mardon, G., Bishop, J. M., and Varmus, H. E. (1988) The first seven amino acids encoded by the v-src oncogene act as a myristylation signal: lysine 7 is a critical determinant. *Mol. Cell. Biol. 8*, 2435−2441.
(46) McLaughlin, S., and Aderem, A. (1995) The myristoyl-electrostatic switch: a modulator of reversible protein-membrane interactions. *Trends Biochem. Sci. 20*, 272−276.
(47) Andersson, H., and von Heijne, G. (1993) Position-specific Asp-Lys pairing can affect signal sequence function and membrane protein topology. *J. Biol. Chem. 268*, 21389−21393.
(48) Seykora, J. T., Myat, M. M., Allen, L. A., Ravetch, J. V., and Aderem, A. (1996) Molecular determinants of the myristoyl-electrostatic switch of MARCKS. *J. Biol. Chem. 271*, 18797−18802.

DOI: 10.1021/bi501134g
Biochemistry 2015, 54, 1111−1122